3.1.4 SIMULTANEOUS VHF AND UHF RADAR OBSERVATION OF THE MESOSPHERE AT ARECIBO DURING A SOLAR FLARE: A CHECK ON THE GRADIENT-MIXING HYPOTHESIS

P. K. Rastogi, J. D. Mathews

Electrical Engineering and Applied Physics Department
Case Western Reserve University
Cleveland, Ohio 44106

and

J. Rottger

Arecibo Observatory
P.O. Box 995
Arecibo, Puerto Rico 00612

INTRODUCTION

The physical mechanism responsible for backward scattering of radio waves from the middle atmosphere depend on the microstructure of small-scale refractivity fluctuations in the vicinity of the Bragg scale, and the spatial distribution (or morphology) of this microstructure within the scattering volume. The electromagnetic part of the scattering process now appears to be reasonably well understood. Characterization of refractivity microstructure, however, is only possible in a statistical sense through simplified models for turbulent gradient-mixing of passive scalars. Such models were originally applied to early tropospheric radio propagation experiments (see e.g. BOLGIANO, 1968), and with slight modification form the basis for the MST radar technique (ROTTGER, 1984). Radar experiments at multiple wavelengths can provide useful information on the refractivity microstructure and its dependence on scales associated with turbulence (BOLGIANO, 1963; RASTOGI and MATHEWS, 1984). Such experiments are feasible only at select facilities.

In this paper, we discuss the results of a two wavelength (VHF and UHF) mesosphere experiment performed at the Arecibo Observatory on January 5, 1981. The 46.8-MHz VHF radar (3.21 m Bragg scale) was operated by the Max-Planck-Institut fur Aeronomie (MPI) to provide spectral measurements of signals scattered from refractivity fluctuations due to turbulence (ROTTGER et al., 1983). Other physical parameters such as radial velocities (V_r), scattered signal power (P_s), and Doppler spread (W_s) due to turbulence can be derived from signal spectra. The 430-MHz UHF radar (0.36 m Bragg scale) was used for D-region electron-density (N) measurements using the incoherent scatter technique with a comparable height resolution (MATHEWS, 1984). The radars were pointed symmetrically about the vertical with a beam spacing of 5.5 degree in the meridional plane. Occurrence of a type 4 solar flare during the experiment produced enhanced D-region electron-density gradients. This was a unique circumstance that provided the possibility of testing the basic premises of the turbulent gradient-mixing hypothesis.

The behavior of physical parameters derived from the VHF experiment is analyzed in the next section. We focus on the evolution of a strong layer of turbulence at 71 km immediately after the flare onset. It is argued that the turbulent layer existed prior to the onset of flare, but was rendered visible through enhanced electron-density gradients established after the onset. Incoherent-scatter electron-density measurements described in Section 3 clearly show substantial enhancement of D-region ionization after the flare. In Section 4, we briefly outline the turbulent gradient-mixing hypothesis. The VHF and UHF observation are then used to show that the development of the layer at 71 km is almost entirely due to enhanced gradients.

VHF OBSERVATIONS DURING THE FLARE

Details of the MPI VHF experiment at Arecibo and the salient results for the December-January 1981 period have been reported by ROTTGER et al. (1983). We review the observations for January 5, 1981, and present the results of further analyses.

Figure 1 shows contours of constant received signal power as a function of height and time. The ST region from 9 to 27 km shows several thin persistent layers. The mesospheric signals are weaker in comparison, but layers in the vicinity of 65, 71, 73, and 77 km can be distinctly seen. The layer at 71 km appears suddenly after 12:16 AST, coincident with the occurrence of the flare, but vestiges of it could be seen even earlier. A weak (1-2 dB) but abrupt enhancement of received signal power at this time occurs at all heights, and is probably due to enhanced solar radio emission seen through a secondary lobe of the antenna radiation pattern (ROTTGER, 1983). Details of flare occurrence are shown in Figure 2.

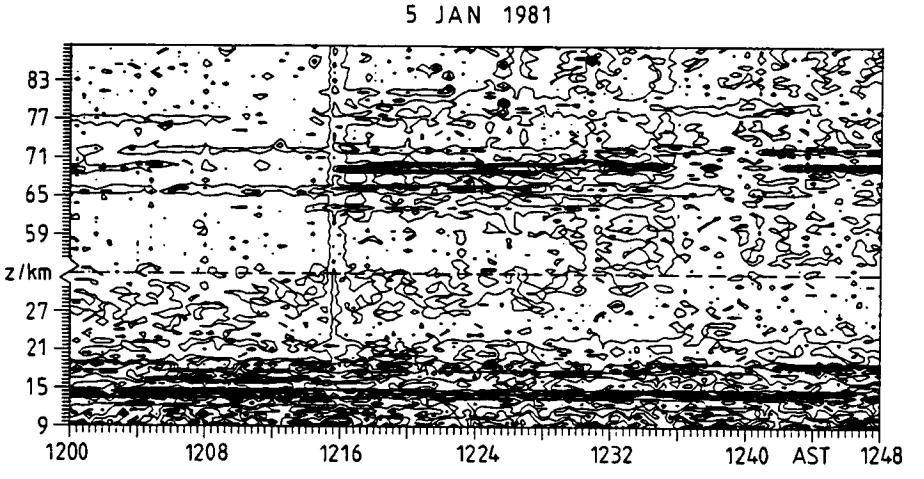

Figure 1. Contour plots of the total received signal power ($P_s + P_n$) at 2 dB increments as a function of height Z and time in AST (UT - 4 hr) for the MPI VHF experiment at Arecibo. Noise enhancement at 12:16 hr AST and subsequent development of the echoing region at 71 km is attributed to the occurrence of a Type 4 Solar Flare. (ROTTGER et al., 1983).

Figure 3 shows the linearly scaled spectra of the received signal and profiles of the noise power P_n, signal power P_s, radial velocity V_r, and Doppler spread W_s in the mesosphere just before and just after the flare onset. A new layer with a near 10 dB enhancement in P_s appears to form at 71 km, but the weak layers at 68 and 73 km do not show any significant variation in the signal power. Enhancement of incoming ionizing radiations (Lyman Alpha and hard X-rays) during the flare cannot produce turbulence, but it can amplify the refractivity structure within an already turbulent layer by creating steeper gradients in the ambient electron densities.

The intensity of turbulence within a layer of thickness L is characterized by the parameter ε denoting the rate at which energy is dissipated per unit mass by turbulence. ε can be related to overturning by buoyancy of the largest eddies (of size L) within the layer. Mean background wind shear produces a

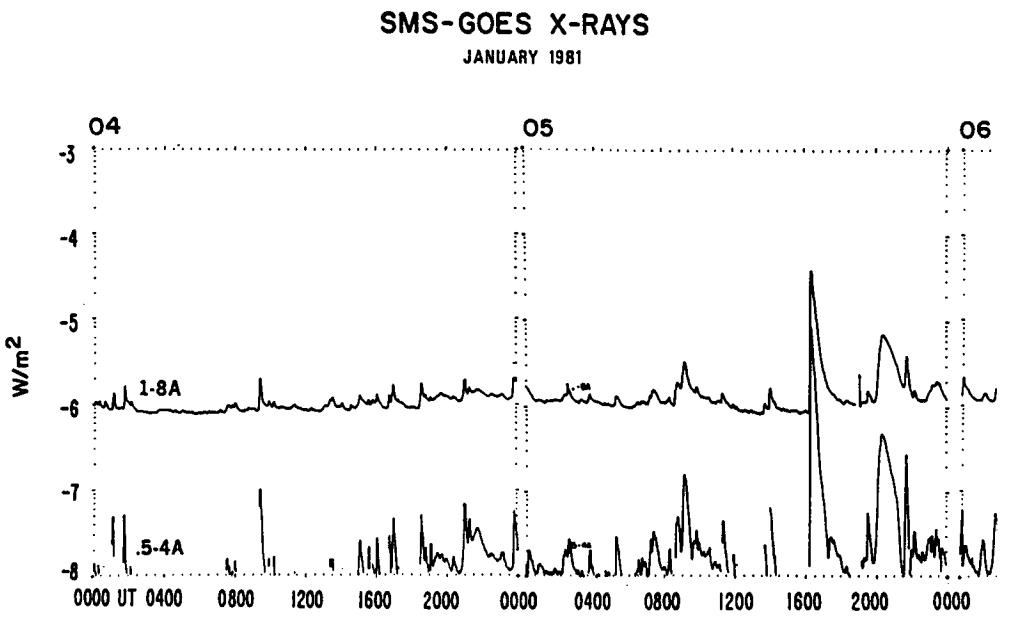

Figure 2. Solar X-ray fluxes in the 1-8 A band (upper) and 0.5-4 A band (lower) recorded by the SMS GOES satellite for January 4-5, 1981. A Type 4 solar flare occurred at 16:13 hr UT (12:13 hr AST) on January 5. It reached a maximum at 16:16:30 hr UT and lasted for 11 min. (Solar-Geophysical Data Comprehensive Reports, No. 443 pt II, July 1981, NOAA).

velocity differential across the layer which is mixed by eddies of successively smaller sizes. The velocity profile in the vicinity of the layer is slightly deformed to maintain a supply of energy to the layer at the rate ε. Details of this process have been considered by LINDEN (1979) and ROTTGER (1981). The distribution of turbulent velocity fluctuations across the layer is mapped into the Doppler spectrum of the scattered signal, and the Doppler spread W_s is linearly related to ε. A small contribution to W_s due to wind shear is negligible for radar pointing directions close to vertical (SATO, 1981).

Figure 4 shows the time evolution of received signal power P_s and Doppler spread W_s in the vicinity of the 71-km layer. At 70.8 km, estimates of W_s (without any noise correction) are slightly less than 1.5 m/s for noise alone. The statistical variation in this parameter is about 0.2 m/s and remains at about the same level for time intervals 11:30-12:15 AST and 12:15-13:00 AST. We conclude, therefore, that the average energy dissipation parameter $\langle\varepsilon\rangle$ remains reasonably constant before, during and after the occurrence of the flare.

ELECTRON-DENSITY MEASUREMENTS

Profiles of electron densities obtained with the incoherent-scatter technique are shown in Figure 5. The time resolution for these measurements is typically 10 min and height resolution is typically 0.5 km. The profiles have been rescaled from total signal power profiles that are smoothed and filtered to remove the effect of external interference. A typical uncertainty in electron-density measurements is of the order of 10 electrons cm^{-3}. The

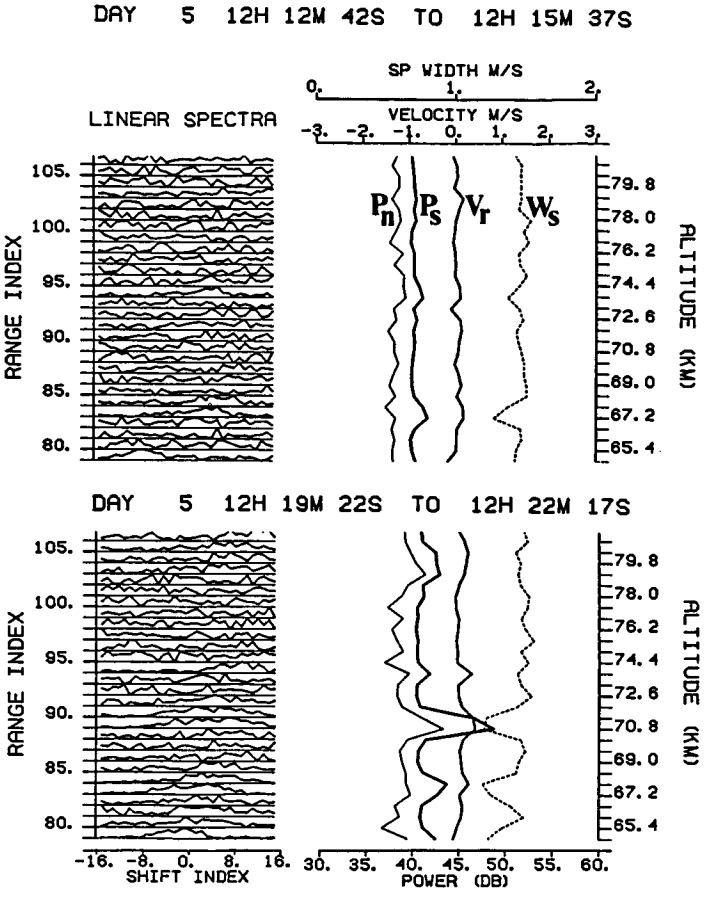

Figure 3. Received signal spectra in the mesosphere, linearly rescaled for each height, are shown on the left for the VHF experiment. Derived parameters P_n, P_s, V_r, and W_s (see text) are shown in the right panels. Top two panels cover the period just before the flare reached its peak. The two lower panels are after the flare peak. Appearance of the layer at 71 km is discussed in the text.

profiles are not obtained at equal time spacing. The actual averaging intervals are tabulated in Figure 5. Profiles 1 and 2 correspond to periods just before and just after the flare onset. Profiles 3 to 5 are for successively later periods. At a height of 71 km, electron density abruptly increases from $\sim$80 cm^{-3} to $\sim$700 cm^{-3} during the first 10 min of the flare, and then gradually decays back to $\sim$100 cm^{-3} over the next half hour. Electron-density gradients dN/dZ in the vicinity of the layer show a local maximum, and a similar pattern of enhancement after the flare onset.

DISCUSSION OF TURBULENT GRADIENT MIXING

The local gradients dN/dZ in electron density N (any passive scalar in general) are mixed by turbulence, producing a spatial power spectrum of fluctuations in N. The scattered signal is obtained as a component of this

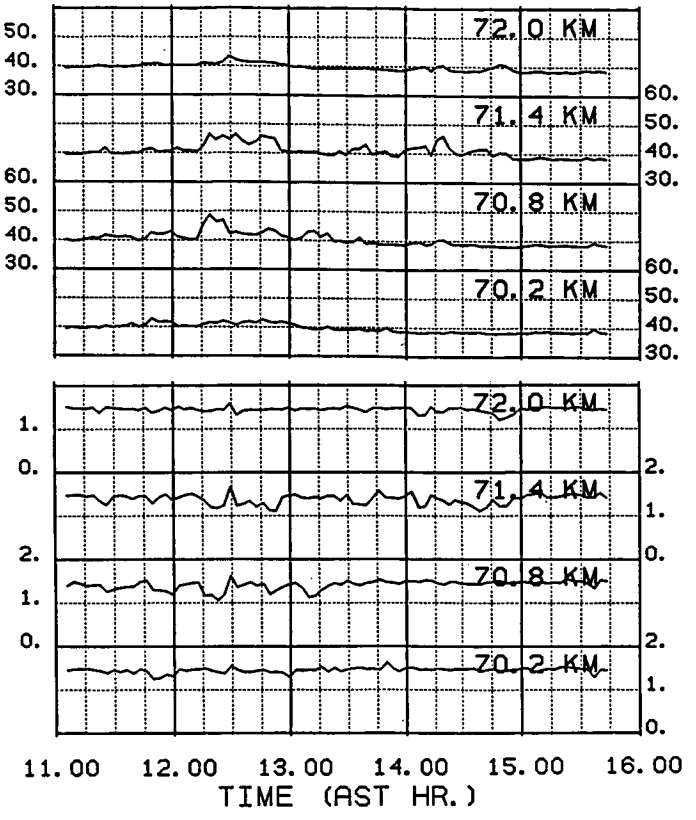

Figure 4. Time variation of total received signal power $P_s + P_n$ (top panel) and Doppler spread W_{s+n} without noise correction (bottom panel). Flare occurs at about 12:15 hr AST. The statistical variation in W_{s+n} is about the same over 11:30-12:15 hr as over 12:15-13:00 for the 70.8 km altitude. For this altitude $P_s + P_n$ jumps by about 9 dB at 12:15 hr.

spatial fluctuation spectrum evaluated at the Bragg wave number. It follows that the scattered signal power P_s would depend on $[dN/dZ]^2$. The energy spectrum of velocity fluctuations that mix the scalar gradient has several (two or more) cutoff scales associated with it. The smallest of these scales depends on the energy dissipation parameter ϵ. The exact wave number dependence of the energy spectrum, hence the wavelength dependence of P_s is decided by the location of Bragg scale in relation to the cutoff scales. RASTOGI and BOWHILL (1976a,b) discuss wavelength dependence of P_s from dimensional considerations. BOLGIANO (1968) and others have pointed out that potential concentrations of the passive scalars should be considered in mixing theories. HOCKING (1983) has derived improved relations for wavelength dependence of P_s in the mesosphere for inertial range turbulence. For discussion of experiments at Arecibo we consider only the $[dN/dZ]^2$ term, since no information can be obtained on wavelength dependence.

On the basis of earlier discussion, we assume that the turbulent layer at 70.8 km has constant thickness L and constant energy dissipation parameter

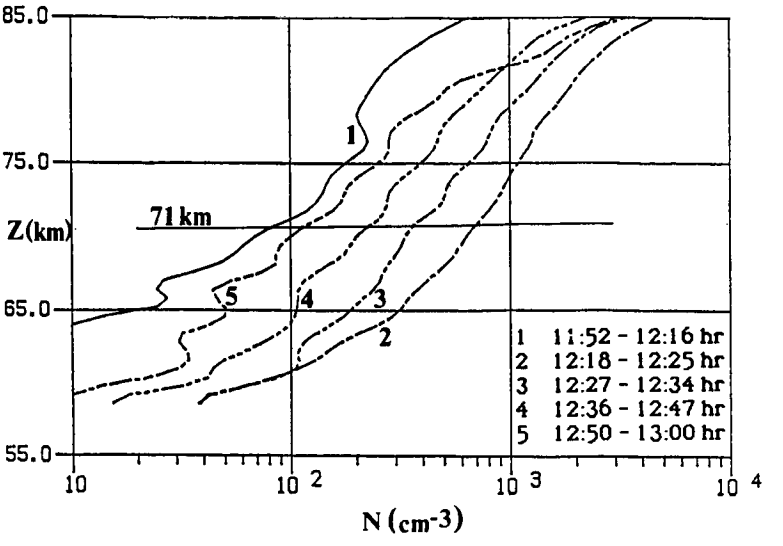

Figure 5. Time evolution of electron-density profiles on January 5, 1981, using the incoherent-scatter technique at 430 MHz. The averaging time corresponding to each profile is shown in the table. For the entire time interval shown, the solar zenith angle remained within 41.0 to 41.6 degrees.

ε for about 0.5 hr before and 0.5 hr after the flare onset. We will consider the following form for the signal power:

$$P_s = A\ F(\varepsilon, L, f_o)\ [dN/dZ]^2 + B$$

where A is a constant, F contains the dependence on ε, layer thickness L, and radar frequency f_o. B is an additive correction term that may be important in more exact formulations using potential quantities. We will assume that B=0.

Figure 6 shows the time variation of the total signal power at 70.8 km in the VHF experiment, and electron-density gradients at 2-km scale derived from the UHF experiment. Suppose that at two closely spaced times t_1 and t_2 signal powers are P_1 and P_2, and gradients are $[dN/dZ]_1$ and $[dN/dZ]_2$. If all other parameters are constant and B=0, then the ratio R given by:

$$R = [P_2\ dB - P_1\ dB]\ /\ 10\log_{10}\{[dN/dZ]_1\ /\ [dN/dZ]_2\}^2$$

should be 10. In applying this test to data of Figure 6, we face the problem that the power and gradients have disparate time scales. This problem can be circumvented by considering transitions in gradients (labeled 1 to 4) and using appropriate values of P_s. The noise level is reasonable constant at 40 dB. For transition 1, we find that R = 8. Transition 2 has only a small change in gradient associated with it, so we combine it with 3. These two transitions give R = 8.7. Transition 4 cannot be used, as a decrease in gradient is associated with enhancement in power. This suggests that the assumption of constant ε and L may have become untenable for intervals exceeding 1 hr.

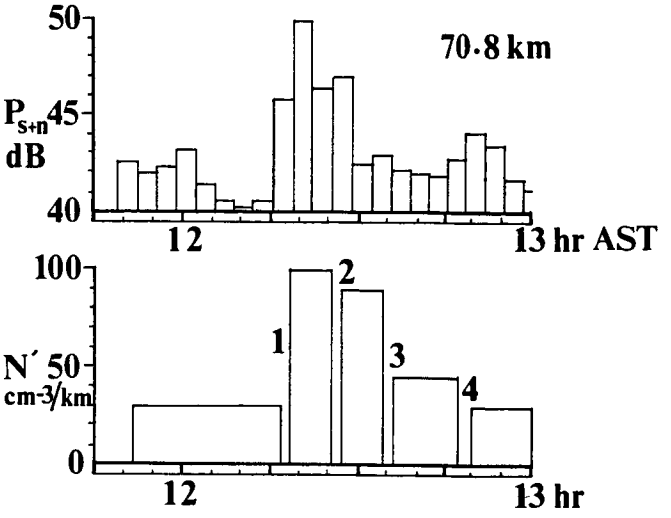

Figure 6. Time variation of the total VHF received signal power P_{s+n} for the 71-km layer at 3 min intervals (upper panel), and the electron-density gradients obtained with the incoherent-scatter method with variable averaging intervals as shown (lower panel). Gradients are obtained with a 2-km scale. Labels 1-4 in the lower panel indicate transitions in gradients that are referred to in the text.

We note that the value of R found in the two cases are both less than and close to 10. This suggests that the assumptions made in our analysis hold reasonably well, and that enhanced electron-density gradients associated with the flare were the principal reason for the layer seen at 70.8 km. A value of R>10 is physically unrealistic as it does not allow dependence on other parameters. The deficit from R=10 can be attributed to following plausible reasons: (a) variability in ϵ, L, (b) local gradients steeper than average gradients, and (c) non-zero additive terms derived from mixing of potential scalars. In view of intermittent nature of turbulence, we expect (a) to be most significant.

ACKNOWLEDGMENT

This work was supported by the National Science Foundation through Grants ATM 8418977 and ATM 8313153. We thank Dr. T. E. VanZandt for useful comments.

REFERENCES

Bolagiano, R. Jr. (1963), The role of radio wave scattering in the study of atmospheric microstructure, in Electromagnetic Scattering, edited by M. Kerker, 261-267, MacMillan, New York.

Bolgiano, R. Jr. (1968), The general theory of turbulence - turbulence in the atmosphere, in Winds and Turbulence in Stratosphere, Mesosphere, and Ionosphere, edited by K. Rawer, 371-400, North Holland, Amsterdam.

Hocking, W. K. (1983), The relationship between strength of turbulence and backscattered radar power at HF and VHF, Handbook for MAP, 9, edited by S. A. Bowhill and B. Edwards, 289-301, SCOSTEP Secretariat, Urbana, Illinois.

Linden, P. F. (1979), Mixing in stratified fluids, Geophys. Astrophys. Fluid Dyn., 13, 3-23.

Mathews, J. D. (1984), Incoherent scatter radar studies of the mesosphere, Handbook for MAP, 13, edited by R. A. Vincent, 135-154, SCOSTEP Secretariat, Urbana, Illinois.

Rastogi, P. K., and S. A. Bowhill (1976a), Radio wave scattering from the mesosphere 2. Evidence for intermittent mesospheric turbulence, J. Atmos. Terr. Phys., 38, 399-411.

Rastogi, P. K. and S. A. Bowhill (1976b), Radio wave scattering from the mesosphere 2. Evidence for intermittent mesospheric turbulence, J. Atmos. Terr. Phys., 38, 449-462.

Rastogi, P. K. and J. D. Mathews (1984), Usefulness of multifrequency MST radar measurements, Handbook for MAP, 14, edited by S. A. Bowhill and B. Edwards, SCOSTEP Secretariat, Urbana, Illinois.

Rottger, J. (1981), The dynamics of stratospheric and mesospheric fine structure investigated with an MST VHF radar, Handbook for MAP, 2, edited by S. K. Avery, 341-349, SCOSTEP Secretariat, Urbana, Illinois.

Rottger, J. (1983), Origin of refractive index fluctuations in the mesosphere as opposed to the stratosphere and troposphere, Handbook for MAP, 9, edited by S. A. Bowhill and B. Edwards, 143-144, SCOSTEP Secretariat, Urbana, Illinois.

Rottger, J. (1984), The MST radar technique, Handbook for MAP, 13, edited by R. A. Vincent, 187-232, SCOSTEP Secretariat, Urbana, Illinois.

Rottger, J., P. Czechowsky, R. Ruster, and G. Schmidt (1983), VHF radar observations of wind velocities at the Arecibo Observatory, J. Geophys., 52, 34-39.

Sato, T. (1981), Coherent radar measurements of the middle atmosphere and design concepts of the MU radar, Ph. D. Thesis, Kyoto University, Japan.